Resistive damping implementation improve controllability in ohmic RF-MEMS switches

M. SPASOS[1], R. NILAVALAN[2]

(1) ATEI of Thessaloniki, Electronics Department, P.O.Box 141, 57400 Sindos, Thessaloniki, GREECE, +30 2310013628
(2) Brunel University, Electronics & Computer Eng. Department, Uxbridge, Middlesex UB8 3PH, London, UK, +44 1895267069

Abstract **- This paper presents in detail the entire procedure in calculating the bias resistance of an ohmic RF-MEMS switch, controlled under resistive damping. (Charge drive technique). In case of a very stiff device, like the North Eastern University (NEU) switch, the actuation control under resistive damping is the only way to achieve controllability. Due to the short switching time as well as the high actuation voltage, it is not practical to apply a tailored control pulse (Voltage drive control technique). Implementing a bias resistor of 33MΩ in series with the voltage source, the impact velocity of the cantilever has been reduced to 13.2 cm/sec from 65.9cm/sec, with only a small increase in the switching time (3.47μs from 1.72μs), eliminating bouncing and high initial impact force during the pull-down phase. During the release phase the amplitude of bouncing has been also reduced to 174nm from 255nm, proving that incorporating resistive damping significant improvement in both switching operation phases of the switch can be achieved.**

I. INTRODUCTION

A reliable ohmic RF-MEMS switch should be capable of switching very fast without the necessity of settling periods due to bouncing phenomena. Additionally, as soon as the switch closes, the contact force should be sufficient and constant. During the release phase, the switch should return to its null position as fast as possible in order to be ready for the next actuation pulse. In reality, there is always a trade-off between switching speed, settling time and contact force. Fast switching under a voltage step pulse, can be achieved by increasing the amplitude of the actuation pulse. Nevertheless, one of the main problems associated with electrostatic actuation under open loop voltage control is the pull-in instability, a saddle node bifurcation phenomenon wherein the cantilever snaps-through to the underneath contact area once its displacement exceeds a certain fraction (typically 1/3) of the full gap. Increased cantilever pull-in velocity implies bouncing and settling time is necessary for the switch to perform its best. Moreover, the contact force during the settling period is not constant, reaching undesirable peak values when the cantilever touches its corresponding contact area for the first time. That results in unstable contact resistance, power loss and arching as far as the signal is concerned and induces local hardening, pitting or dislocations in the metal crystal structures of the materials used, reducing the reliability and the longevity of the switch [1]

II. RESISTIVE DAMPING

Instead of using a continuous step command to control the switch, a tailored pulse with different levels of applied voltages and time intervals can be applied. In the past few years several efforts have been made to tailor the shape of the actuation pulse while recent publications presented accurate solutions achieving remarkable results [2]-[5].

Nevertheless, tailored pulse (voltage control) techniques can be applied only in relatively slow switches with switching time Ts ≥ 10μs and actuation voltage Vs ≤ 60V, allowing enough time for an efficient pulse train to be formed.

Another way to control the impact velocity achieving soft landing and fewer bouncing phenomena is the resistive damping. This control method is also referred as charge drive and has been presented for the first time by Castaner and Senturia [6]. Under charge control the pull-in phenomenon of the Constant Voltage controlled electrostatic actuators does not exists while, if the current drive is ideal, any position across the gap is stable. The main reason for this behavior is that the applied electrostatic force is always attractive and is independent of the remaining gap of the actuator.

Charge drive control using constant current sources is mostly preferred to extend the travel range of electrostatic micro-actuators [7], [8]. Nevertheless, there are very few references in the literature as regards charge drive control on RF MEMS. Among them, a paper based on numerical simulations for a capacitive RF-MEMS by Lee and Goldsmith [9] and another one recently published, by Blecke et al [10], which presents a learning algorithm for reducing fabrication variability using resistive damping for the pull-down phase. None of these papers present any details on how to implement resistive damping or any results of such kind of applications. Varehest et al [11], attempted to control the bouncing of a MEMS accelerometer at its resonance frequency using a single resistor.

In case a constant voltage source V increases, the electrostatic force is increased due to the increase in the charge (Q).

$$F_e = \frac{QV}{2g} \quad (1)$$

Simultaneously, the increased force decreases the beam height (g), which, in turn, increases the capacitance and its charge. In other words the electrostatic energy provided by a constant voltage source V, is converted to kinetic energy, accelerating the beam [7].

$$E_k = \frac{mv^2}{2} \quad (2)$$

At $g=2/3g_0$, the increase in the electrostatic force is greater than the increase in the restoring force, resulting to an unstable condition and a collapse of the cantilever beam to the CPW line. This behavior creates a high impact force and bouncing phenomena.

$$V_C = V_S\left(1 - e^{-\frac{t}{RC}}\right)V_C \quad (3)$$

When a voltage source with a large series bias resistance is used instead, the behavior of the switch is not the same. The presence of the high bias resistor changes the behavior of the source, to a rather constant capacitor current charge, which mainly depends on the resistor's value. Under these conditions the source behave like a current source and reduces the kinetic energy of the MEMS switch near the point of contact by causing the voltage across the switch to drop in case of a rapid change in the capacitance of the electrode area.
Under these conditions the constant charging current of the capacitor which is created under resistive damping between the electrode area and the cantilever during the transition time of the actuation pulse is given by:

$$i_c = C\frac{\Delta t}{\Delta V_c} \quad (4)$$

And for the case of an ohmic cantilever type switch is transformed as:

$$i_c = C_{el}\frac{t_{in}}{V_c} \quad (5)$$

where:
C_{el} is the capacitance between the electrode and the cantilever in its initial position.
V_C is the maximum voltage of the actuation pulse
t_{in} is the inertia time of the cantilever when a ramp voltage is applied (rise time of the pulse).

The value of the appropriate bias resistance for reducing the velocity of the cantilever is calculated as:

$$(5) \Rightarrow \frac{V_C}{I_C} = \frac{t_{in}}{C_{el}} \Rightarrow R_B = \frac{t_{in}}{C_{el}} \quad (6)$$

As is shown from the (6) the R_B is independent from the amplitude of the actuation pulse and is depended only of the quotient of the inertia time of the cantilever (t_{in}) by the C_{el}.
Such a bias resistance cause soft landing with less bouncing phenomena, lower initial impact force but it also introduces additional delay to the switching time.
All the above considerations are valid only for the case that the rise time (t_r) of the pulse is smaller than the switching time $t_r < t_s$, which means that during the rise time of the pulse the cantilever has not started to move yet and its initial capacitance remains stable.
For series ohmic RF-MEMS switches the capacitance created by the electrode area of switches in the up state is in the order of 0.02 to 1pF, with a final remaining gap of $g > 0.4\mu m$ in the down-state position. The current drown out of the source by the variable capacitor during the transition time is very small (2–20 μA) and a bias resistance R_B = 10–50MΩ is needed for an appreciable voltage drop.
To eliminate bouncing phenomena, during the release phase of the switch, when the cantilever oscillates in the resonance frequency, the R_BC_{el} product must be equal to the period of the resonance frequency (t_{res}) [11] and the R_b for this case is calculated as:

$$R_B = \frac{t_{res}}{C_{el}} \quad (7)$$

III. APPLYING RESISTIVE DAMPING TO IMPROVE CONTROLABILLITY

The ohmic RF-MEMS switch which is under examination is based on the exact dimensions of NEU switch as have been published by Guo at al [12] and shown in Fig. 1. The first version of this switch has been designed and developed by the Professors McGruer and Zavracky at North-Eastern University (NEU) in conjunction with Analog Devices and fabricated at Radant Technologies.. Moreover the published measurements of the "NEU" switch will be used in order to validate the simulation process that will be followed for the next design.

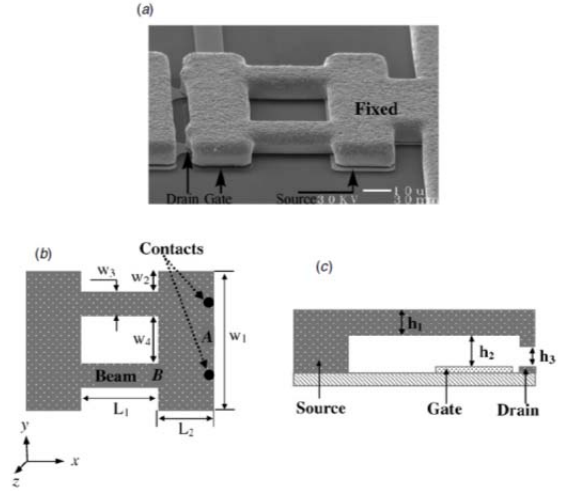

Fig. 1. (*a*) SEM micrograph of the "NEU" switch. (*b*) Top and (*c*) Side views of the switch, where w_1=80μm, w_2=10μm, w_3=16μm, w_4=30μm, L_1=30μm, L_2=24μm, h_1=6μm, h_2=0.6μm and h3=0.38μm.

At first a manufacturing process and a 2D model for the switch based on the above dimensions is created under Designer modulus and then transformed in 3D under Analyzer modulus as shown in the meshed design of Fig.2.

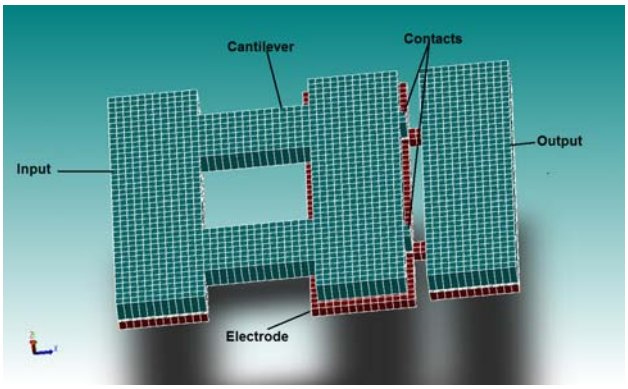

Fig. 2. The "NEU" ohmic RF MEMS switch

Top and bottom views of the modelled "NEU" switch (expanded 2 times in z axis) under actuation voltage (ON state), are presented in Fig. 3 & 4.

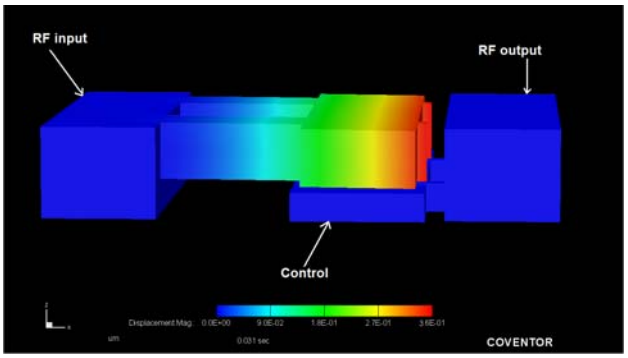

Fig. 3. Top view of the "NEU" ohmic RF MEMS switch

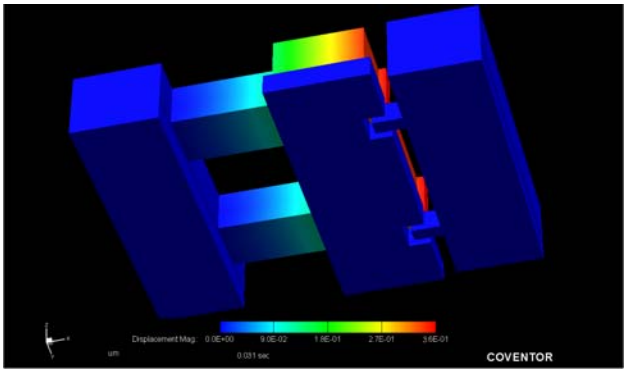

Fig. 4. Bottom view of the "NEU" ohmic RF MEMS switch

DC Transfer Analysis

A DC transfer analysis via Architect module has been carried out by applying a ramp voltage to investigate on: actuation voltage, contact force, conductance, contact area and capacitance as shown in Fig. 5. All the design parameters of the "NEU" switch are illustrated in Table 1

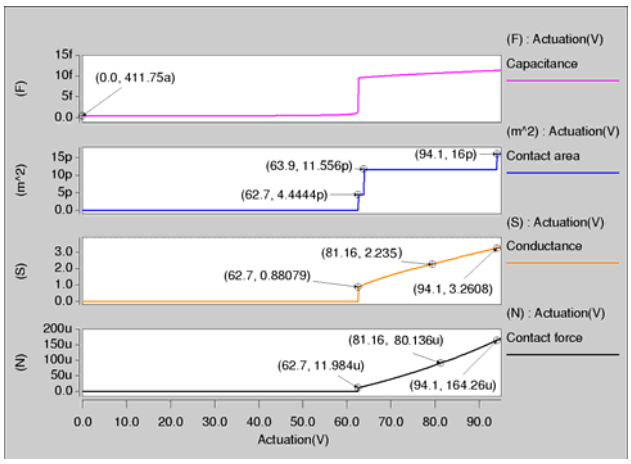

Fig. 5. DC analysis results of the "NEU" switch

Table 1. Design parameters of the "NEU" switch

Parameter	Value	Parameter	Value
Length (total) 2XCantilever Actuation pad	54μm 30μm 24μm	Contact force	11.98μN (V_{arc}) 80.136μN(V_s) 164.26μN($V_{s(max)}$)
Width 2XCantilever Actuation pad	 16μm 80μm	Conductance	0.88S (V_{arc}) 2.235S ($V_{s(nom)}$) 3.26S ($V_{s(max)}$)
Height from electrode	0.6μm	Pull-in (V_p) First contact(V_{arc}) Full contact($V_{s(min)}$) Nominal (V_s) Maximum ($V_{s(max)}$)	60.2V 62.7V 63.9V 81V 94V
Height from contacts	0.38μm	Capacitance (OFF)	0.822fF
Cantilever Type	Gold	Rayleigh gas damping parameters	α=406083/s β=0μs
Cantilever thickness	6μm	Q_{GAS}	5.31
Holes to cantilever	No	Contact Area	11.556pm^2

Transient Analysis

A transient analysis is performed first under step pulse implementation with 81V amplitude, width p_w = 48μs, rise time t_r = 2μs and fall time t_f = 2μs. The amplitude of 81V is chosen so, to be direct comparable with this of "NEU" switch presented by Guo at al [108]. As well as the rise time of the actuation pulse is chosen to be less than 50V/μs, in order to avoid transient phenomena which have been observed in the laboratory for faster transitions.

The switching time which is obtained under the above pulse conditions, was around 2.48μs for the OFF-ON transition and around 1.73μs for the OFF-ON transition, as shown in Fig. 6. This figure shows the fastest ON and OFF switching time that can be achieved. Besides, the same figure illustrates the bouncing problems during the pull-down (max. bounce = 174μm) and release (max. bounce = 255μm) phases. High settling times are observed also due to the stiffness of the cantilever (k ≈ 1000 N/m), which are around 11μs for the pull-down phase and around 39μs for the release-phase.

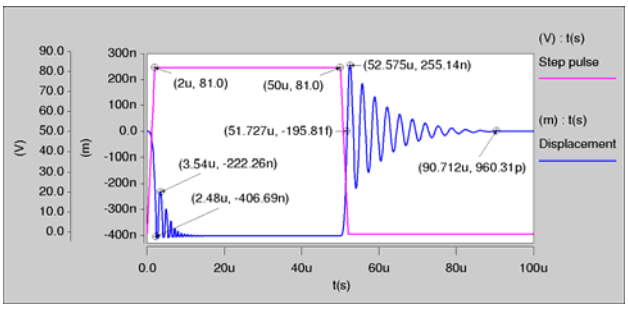

Fig. 6. Displacement under step pulse implementation

Fig. 7 illustrates the other characteristics of the switch under step pulse implementation, such as, contact area (11.566pm^2), conductance per contact area (2.235S which corresponds to a resistance of 0.447Ω) and contact force (80.153μN).

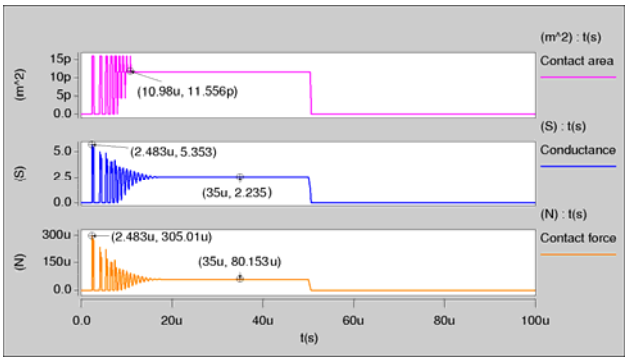

Fig. 7. Characteristics of the switch under step pulse implementation

A comparison between the simulations and measurements [12], as illustrated in Table 2, shows good agreement between the published measured and simulation results.

Table 2. Comparison between simulations and measurements

Parameter	NEU (simulations)	NEU (measurements)
V(arc)	63.9V	63V-66V
V(pulse)	81V	81V
Switching time	2.48μs	1.24μs
Resonance frequency	339kHz	346kHz
Initial bounce	222nm	200nm
Number of bounces during Pull-in phase	8	8
Initial contact force	305μN	320μN
Static contact force	80μN	78μN

The differences in switching time (t_s) depends on the rise time (t_r) of the actuation pulse, this feature was not defined in the published paper. Simulations with t_r = 1μs showed t_s =1.7μs, while with t_r = 2μs as in the previous study showed t_s = 2.48μs.

Control under Resistive Damping

Another transient analysis was performed next under step pulse implementation with resistive damping, with 81V amplitude, width p_w = 48μs, rise time t_r = 2μs and fall time t_f = 2μs. The damping resistance can be calculated as:

$$R_B C_{el} = t_r = 2\mu m \Rightarrow R_B \approx 66M\Omega \quad (8)$$

where: C_{el}=30fF, the capacitance which is created within the electrode area.

However, the switching time has been simulated to be around 2.4μs, which means that for t=2μs the cantilever has been moved and the C_{el} is much larger as the distance from the electrode has been reduced. According to the simulated results of Fig.6, the cantilever remains in the initial condition for about 1μs before starts to bend and this inertia time will be used for the calculation of the correct damping resistance:

$$R_B C_{el} = t_r = 1\mu m \Rightarrow R_B \approx 33M\Omega \quad (9)$$

The results in Fig. 3.8 show the difference between these two cases with respect to displacement and contact force. The simulation results with R_b = 33MΩ shows excellent response of the switch during the pull down phase as they show elimination of the bouncing and the initial impact force (the high impact velocity has been reduced to 13.2 cm/sec from 65.9cm/sec), with only a small increace in the switching time (4.34μN from 2.38μN). During the release phase a significant reduction in bouncing is also observed (169nm from 255nm).

The results with R_b = 66MΩ also shows elimination of the bouncing and the initial impact force, however with a significant increace in the switching time (7.32μN from 2.38μN) and the initial settling time. During the release phase, a better response is observed (52nm from 255nm), as the time constant RC = 2μs is very closer the period of the resonance frequency of the cantilever t_{res} = 2.9μs.

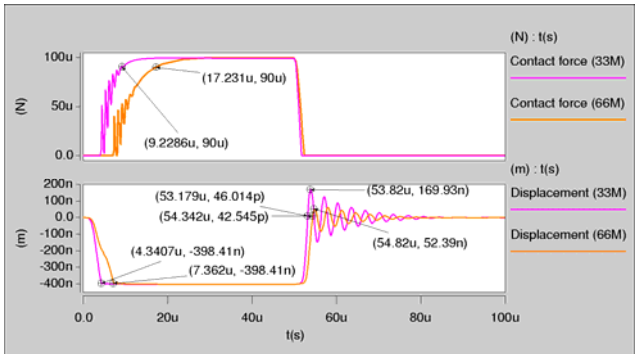

Fig. 8. Characteristics of the switch under different damping resistors

Under the above considerations the R_B = 33MΩ has been chosen for further analysis of the switch as shown in Fig.9

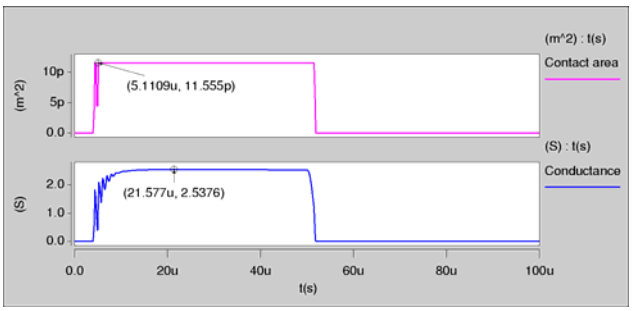

Fig. 9. Contact area and conductance of the switch with $R_B = 33M\Omega$

Hot Cycling Mode of Operation

This section presents the results from the new switch under hot cycling mode of operation, where the RF signal is passing through during the ON-OFF operation of the switch. Fig. 10 shows the displacement of the cantilever and the output of the switch when an RF signal with amplitude of 1V and frequency of 2GHz is applied at the input under step pulse actuation.

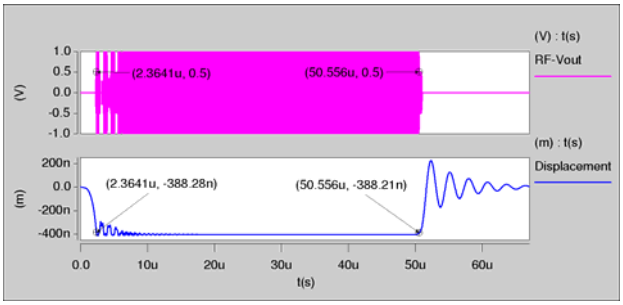

Fig. 10. Behaviour of the switch under step pulse actuation

In order to handle the bouncing problems which are created under step pulse excitation, resistive damping can be used. Fig. 11 shows the displacement of the cantilever under resistively damped step pulse (damping resistance $R_B = 33M\Omega$) and the RF output of the switch when an RF signal with amplitude 1V and frequency of 2GHz is applied, in time correlation.

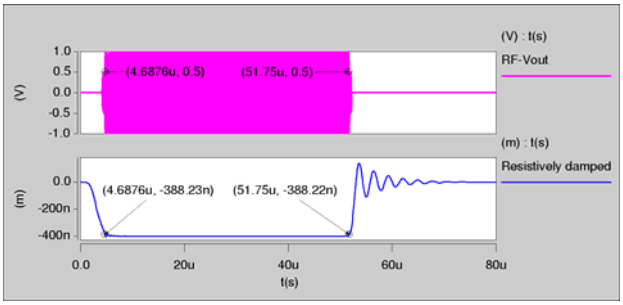

Fig. 11. Behaviour of the switch under hot mode of operation

Fig. 12 shows the behaviour of the cantilever when RF signals with amplitude of 10V, 45V and 100V are applied together with the resistive damped step pulse. It is obvious that the bouncing of the cantilever increases depending on the RF signal amplitude. For RF signal amplitudes higher than 45V the release time of the cantilever is increased to 5μs as a consequence of V_{DC} = 63V, which is equal to the V_{arc} = 63V voltage of the switch.

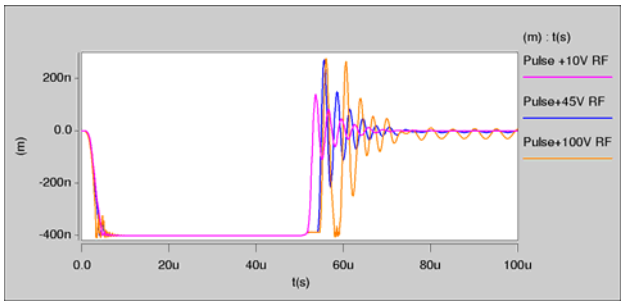

Fig. 12. Displacement under the influence of various RF signals

Electromagnetic Analysis

A full electromagnetic wave analysis has been carried out to further investigate the S-parameters of the switch using the two-port analysis from the Architect module. The characteristic impedance Z_0 for input and output is set at 50Ω. Fig. 13 presents the Isolation and Return loss graphs in the frequency range of DC to 20 GHz, when the switch is in the OFF state. The simulation results are excellent as the values of the Isolation and Return Loss are -51.5dB and -0.000031dB, respectively, at 5 GHz.

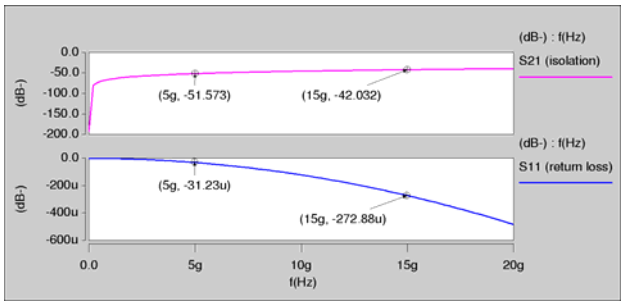

Fig. 13. Isolation and Return loss graphs of the "NEU" switch in the OFF state

The behaviour of the switch is further investigated with the switch in the ON state presenting significant results with Return loss -48.77dB and Insertion loss -0.018dB at 5GHz. The results of the simulation in the frequency range DC-20GHz are illustrated in Fig. 14.

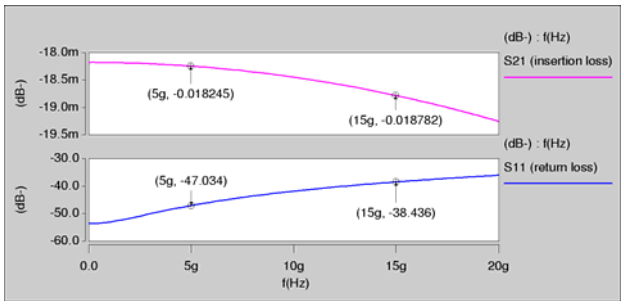

Fig. 14. Insertion and Return loss of the "NEU" switch in the ON state

A summary of the simulated parameters of the "NEU" in line series ohmic RF-MEMS switch is presented in Table 3.

Table 3.3. Performance results "NEU" switch under resistive damping actuation

Parameter	Value
Pulse amplitude	83V
RF signal (max)	45V
Contact force	99.286μN
Conductance	2.537S
Switching Time	4.34μS (OFF-ON) 3.179μS (ON-OFF)
Isolation (OFF) (S21_5GHz)	-51.5dB
Return loss (OFF) (S11_5GHz)	-0.000031 dB
Insertion loss (ON) (S21_5GHz)	-0.018 dB
Return loss (ON) (S11_5GHz)	-47 dB
SNR	83.7dB_OFF 60.9dB_Trantition 81.6dB_ON

IV. CONCLUSION

A quantification of the existing method of resistive damping (charge control) has been presented, which allows the exact calculation of the bias resistor needed for resistive damping to be applied. This technique reduces impact force during the pull-down phase as well as bouncing during the release phase. Evaluating the "NEU" switch incorporating resistive damping, significant results have been extracted. This type of switch is very stiff and presents very low switching time as well as high mechanical resonance frequency. These characteristics allow the implementation of a bias resistor capable of improving switching performance in both phases. It has to be mentioned that for this type of stiff switches, resistive damping is the only adequate control technique since practically there is not enough time for tailored pulse to be implemented.

REFERENCES

1. H. Newman, et al, "Lifetime Measurements on a High-Reliability RF-MEMS Contact Switch", *IEEE*, *Microwave and wireless component letters,* 2008, Vol. 18, pp. 100-102.
2. D. Czaplewski, et al, "A Soft-Landing Waveform for Actuation of a Single-Pole Single-Throw Ohmic RF-MEMS switch", *IEEE, Journal of Microelectromechanical systems, 2006,* Vol. 15, pp. 1586-1594.
3. K. Ou, et al, "A command shaping approach to enhance the dynamic performance and longevity of contact switches", *Elsevier, Journal of Mechatronics,* 2008, pp. 375-389.
4. K. Ou, et al, "Fast Positioning and Impact Minimizing of MEMS, Devices by Suppression of Motion-Induced Vibration, by Command-Shaping Method", *IEEE, Journal of Microelectromechanical systems, 2006,*Vol. 20, no. 1, 2011, pp. 128-139.
5. M. Spasos, et al, "RF-MEMS Switch actuation pulse optimization using Taguchi's method", *Springer, Journal of Microsystems Technologies*, 2011
6. L. Castaner and S. Senturia, Speed-Energy Optimization of Electrostatic Actuators Based on Pull-In, *"IEEE, Journal of Microelectromechanical Systems"*, September 1999, Vol. 8, pp. 290-298.
7. L. Castaner, et al, "Analysis of the extended operation range of electrostatic actuators by current-pulse drive", *Elsevier, Journal of Sensors and actuators,* 2001, Vol. 90, pp. 181-190.
8. R. Nadal-Guardia, et al, "Current Drive Methods to Extend the Range of Travel of Electrostatic Microactuators Beyond the Voltage Pull-In Point", *IEEE, Journal of Microelectromechanical Systems,* 2002, Vol. 11, pp. 255-263.
9. J. Lee and C. Goldsmith, "Numerical simulations of novel constant-charge biasing method for capacitive RF MEMS switch", *In Proceedings of NanoTech Conference*, San Francisco, USA, 2003. pp.396-399.
10. J. Blecke, et al, "A Simple Learning Control to Eliminate RF-MEMS Switch Bounce", *IEEE, Journal of Microelectromechanical Systems,* 2009, Vol. 18, pp.458-465.
11. M. Varehest, et al, "Resistive Damping of Pulse-Sensed Capacitive Position Sensors", *TRANSDUCERS '97, international Conference on Solid-state Sensors and Actuators, IEEE*, Chicago, USA, June 16-19, 1997.
12. Z. Guo, et al, "Modeling, simulation and measurement of the dynamic performance of an ohmic contact, electrostatically actuated RF-MEMS switch", *IOP, Journal of micromechanics and microengineering,* 2007, pp. 1899-1909.